Left Ventricle Segmentation in LGE-MRI: Filter Based vs. Learning Based

Tanja Kurzendorfer, Katharina Breininger, Stefan Steidl, Alexander Brost, Christoph Forman, and Andreas Maier

***Abstract*—Ischaemic heart disease is the number one cause of death world wide, which is in close relation with heart failure. If patients suffer from drug-refractory heart failure with a reduced ejection fraction, cardiac resynchronization therapy is a treatment option. For planning the procedure, precise information about the left ventricle's anatomy and scar distribution is required. The clinical gold standard to visualize scar is late gadolinium enhanced magnetic resonance imaging (LGE-MRI). The challenge arises in the myocardium segmentation of these sequences which is a pre-requisite for an accurate scar quantification. In this work, we compare a filter based approach against a learning based approach for LGE-MRI segmentation. For both approaches the segmentation workflow consists of four major steps. First, the left ventricle is detected. Second, the blood pool is estimated. Third, the endocardium is refined using scar information. Fourth, the epicardium is extracted.**

The proposed methods were evaluated on 100 clinical LGE-MRI data sets. For the learning based approach a 5-fold nested cross-validation is applied to evaluate the hyper-parameters. The learning based segmentation achieves slightly better results, with a Dice score of 0.82 $\pm$ 0.09 for the endocard and 0.81 $\pm$ 0.08 for the epicard.

I. Introduction

Cardiac disease is the major cause of death world wide [1]. In more detail, ischaemic heart disease is the number one cause of death. Ischaemic heart disease is in close correlation with heart failure (HF). According to Dickstein et al. [2] at least 51 % of patients that suffer from HF have an ischaemic history. For diagnosis in clinical routine, cardiac magnetic resonance imaging (MRI) is performed. If patients suffer from a drug-refractory HF, with a reduced left ventricular ejection fraction caused by an asynchronous contraction pattern of the heart, cardiac resynchronization therapy (CRT) is an important treatment option. However, 30 % to 40 % of the patients do not benefit from this therapy [3]. One reason is the suboptimal placement of the left ventricular lead. If the lead is placed on scar tissue, there may be no response. Therefore, knowledge about the left ventricle's anatomy and scar tissue distribution is very important for procedure planning and guidance.

The clinical gold standard for tissue characterization is late gadolinium enhanced (LGE) MRI [4]. For this sequence, a gadolinium based contrast agent is injected intravenously. The images are acquired 10 min to 20 min after the contrast injection. The contrast agent accumulates in the damaged tissue, because of a larger extra-vascular, extra-cellular volume, and a slower washout [5].

T. Kurzendorfer, K. Breininger, S. Steidl, and A. Maier are with the Department of Computer Science, Pattern Recognition Lab, Friedrich-Alexander University Erlangen-Nuremberg, Erlangen, Germany.

T. Kurzendorfer, A. Brost, and C. Forman are with Siemens Healthcare GmbH.

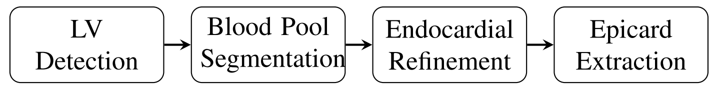

Fig. 1: Overview of the LV segmentation workflow. First, the LV is detected. Second, the blood pool is segmented by applying a morphological active contours approach without edges. Third, the endocardial border is refined using a filter based or learning based approach. Fourth, the epicardial contour is extracted.

The challenge arises in the segmentation of these sequences because of inhomogeneous contrast distribution within the myocardium. Most work in literature use cine MRI images for the segmentation and then propagate the contours to the LGE-MRI images [6], [7], [8]. However, the direct segmentation of the LGE-MRI is desired to achieve an accurate scar quantification.

In this work, we compare a filter based (FB) [9] vs. a learning based (LB) [10] algorithm for the segmentation of the left ventricle (LV) in LGE-MRI.

II. Methods

The LV segmentation pipeline considered in this manuscript consists of four steps [9], [10]. First, the LV is detected in the short axis (SA) stack. Second, the result is used to initialize a morphological active contours without edges (MACWE) approach for initialization of the blood pool [11]. Third, the endocardial contour is refined using either a FB or a LB approach in combination with a minimal cost path (MCP) search in polar space. Fourth, the epicardial boundary is extracted using also either the FB or the LB approach. An overview of the segmentation work flow is given in Figure 1.

1) Left Ventricle Detection: The LV is detected in the mid-slice of the LGE-MRI SA stack, because in this slice the LV has the most circular shape. For the detection, circular Hough transforms are applied in combination with a roundness measure. If the center from the circular Hough transform and the center from the roundness measure are within a certain range, the LV is detected successfully [10].

2) Blood Pool Segmentation: Next, a MACWE approach is applied for blood pool estimation [11]. This approach uses morphological operations instead of partial differential equations, as they are computational efficient and less sensitive to the initialization. The contour evolution depends on the intensity values inside and outside of the contour [9].

978-1-5386-8495-5/18/$31.00

3) Endocardial Refinement: After a rough outline of the blood pool is obtained, the endocardial contour can be refined either using a filter based approach [9] or a learning based method [10]. For both segmentation approaches, a cost map in polar space is derived, where a minimal cost path in polar space is initialized. The cost path finds the distance weighted shortest path from the left side of the images to the right side of the image.

For the filter based approach, the cost array is based on an edge image generated using the Canny edge filter.

For the learning based approach, a random forest classifier trained on steerable features is used to obtain the boundary probability for each potential candidate [10]. Steerable features are low level features based on the local gradient and intensity.

In addition, for both approaches a scar threshold is estimated. Therefore, the mean intensity μ and the standard deviation σ of the blood pool are estimated. The scar threshold is defined as $\theta = \mu + \sigma$. All pixels, that are above this threshold and outside of the blood pool are defined as potential scar candidates.

The final cost array is derived from the cost array combined with the scar map. The MCP finds the distance weighted minimal path. Next, the result is transferred back to the Cartesian coordinate system and the convex hull is taken to exclude papillary muscles and to obtain a smooth looking contour.

After the first contour is refined, the information about the location of the left ventricle is propagated in the basal and apical direction and used for initialization of MACWE approach [11].

4) Epicardial Refinement: For the epicardial contour extraction, the previously estimated endocardial contour is used as an initialization. As for the endocardial refinement, either a filter based approach [9] or a learning based method [10] can be used for the epicardial boundary delineation. For both approaches, the endocardial contour is enlarged by a certain radius and the refinement is performed in polar space.

For the filter based segmentation, the previously calculated edge image is used, and all edges within the enlarged endocardial contour are deleted. Having the modified edge array, the closest edge to the enlarged endocardial contour within a certain margin is searched for.

For the learning based approach, potential boundary candidates are extracted based on the enlarged endocardial contour. For the boundary probability estimation also steerable features are used. After the cost map is obtained, a MCP search is initialized, as for the endocardial boundary estimation.

The final contour is transferred back to Cartesian coordinates and the convex hull is estimated to obtain a smooth contour. The refinement of the epicardial contour in the apical and basal direction ends with the same slice as for the endocardial contour refinement.

III. Evaluation and Results

The automatic segmentation of the LV endocardium and epicardium was evaluated on 100 clinical 2-D LGE-MRI data sets from individual patients. The inversion recovery

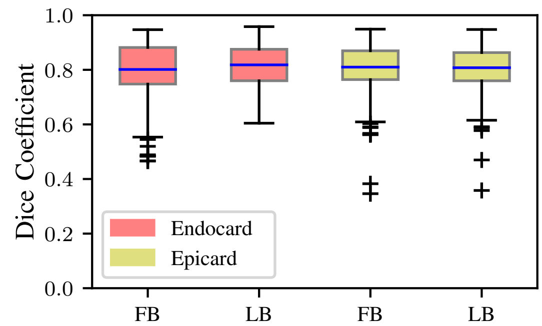

Fig. 2: Comparison of the DC between the FB and the LB segmentation for the endocardium and the epicardium.

LGE-MRI sequences were acquired with a 1.5T clinical scanner (MAGNETOM Aera, Siemens Healthcare, Erlangen, Germany). The slice thickness was set to 8 mm, with a pixel size of (1.59-2.08 $\times$ 1.59-2.08) mm^2 and the spacing between the slices was set to 10 mm. Each data set contained between 10 and 13 SA slices. Gold standard annotations of the LVs endo- and epicardium were provided by two clinical experts. The clinical experts were asked to outline the endocardial and epicardial border separately. To evaluate the overlap between the segmentation results and the gold standard annotations, the Dice coefficient (DC) was used as a quantitative measure of the segmentation accuracy. In addition, the average surface distance (ASD) in mm was evaluated.

For the evaluation of the learning based segmentation, a 5-fold nested cross-validation was performed. Hence, in each fold 20 data sets were used for testing and the rest was used for the training and validation of the classifier. A grid search was applied to optimize the hyper-parameters such as number of trees and the tree depth.

In Table I, the results of the two segmentation methods are presented, using DC and ASD. In Figure 2, the DC of the FB vs. the LB approach are compared, for the endocardium and epicardium, respectively. The blue line represents the mean Dice coefficient. It can be seen that the LB segmentation slightly outperforms the FB segmentation and is more robust against outliers, especially for the endocardium. However, there is no big difference in the final result, as the convex hull is applied for both methods. The qualitative results are presented in Figure 3. The first row depicts the raw data from apex to base. The second row shows the gold standard annotation of the clinical expert, where the endocardial contour is shown in orange and the epicardial contour in green. The third row depicts the result of the filter based approach, where the endocardium is red and the epicardium yellow. The last row visualizes the results for the learning based method using the same colors as for the filter based segmentation. The biggest difference compared to the gold standard annotation appear in the base and the apex, especially for the epicard.

The proposed approaches were implemented in Python and required less than 10 seconds for the segmentation of one sequence on a computer equipped with an Intel i7-4810MQ with 2.8 GHz CPU and 16 GB of RAM.

	Dice		ASD [mm]	
	Filter	Learning	Filter	Learning
Endo	0.80 ± 0.11	0.82 ± 0.09	3.71 ± 2.57	3.73 ± 2.17
Epi	0.81 ± 0.09	0.81 ± 0.08	4.33 ± 2.65	4.39 ± 2.19

TABLE I: Segmentation results for the endocardium (Endo) and epicardium (Epi) evaluated using Dice coefficient and average surface distance (ASD).

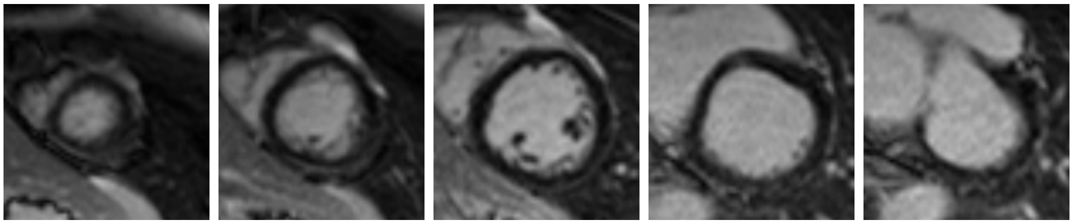

(a) Pseudo SA slices from apical to basal direction

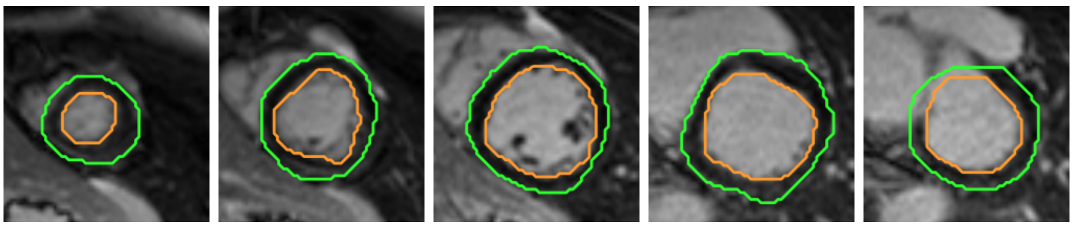

(b) Gold standard annotation from the clinical expert

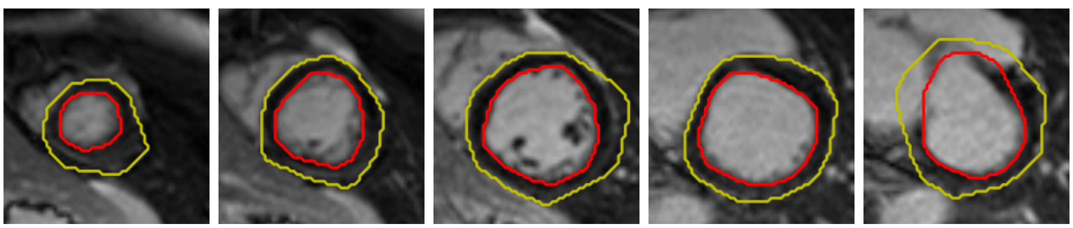

(c) Filter based segmentation result

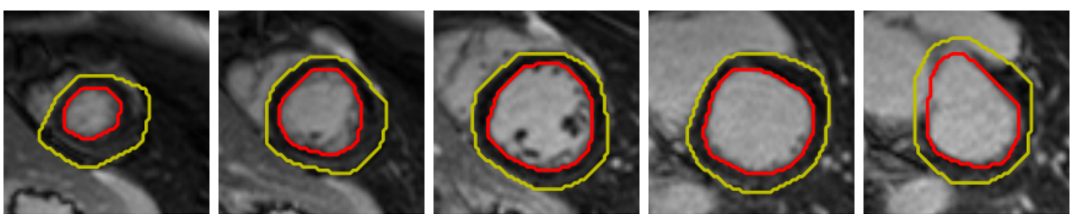

(d) Learning based segmentation result

Fig. 3: Comparison of the segmentation result for the learning based and filter based method. The first row shows the pseudo SA slices from apical to basal direction without any contours. The second row depicts the gold standard annotation from the physician, where the endocardium is marked in orange and the epicardium in green. The third row visualizes the filter based segmentation method where the endocardial contour is shown in red and the epicardial contour in yellow. The fourth row delineates the learning based algorithm, with the same colors as for the filter based approach.

IV. Discussion and Conclusion

Both presented segmentation algorithms only use the LGE-MRI data for the segmentation of the left ventricle. As previously mentioned, most work in literature use cine MRI images for the segmentation and then propagate the contours to the LGE-MRI images [6], [7], [8]. Still, even though we only use the LGE-MRI sequence, our presented results are comparable to the results reported in literature.

The biggest errors occur in the apex and at the left ventricular outflow tract (LVOT). The delineation of the left ventricular outflow tract is not always clear and also depends on the initialization of the short axis scan. The poor performance of ASD is mainly due to the large errors in the apex and at the LVOT. However, the results in the mid-cavity look promising.

In the course of this work, two fully automatic approaches for the left ventricle segmentation in LGE-MRI have been presented, that provide accurate and consistent results. A clear benefit of the presented methods is the independence of the cine MRI contour propagation. The proposed LB segmentation achieves slightly better results when compared to the FB method, especially in the mid-cavity and is more robust against outliers. For future work, different post-processing methods will be considered. Furthermore, a graph-cut based approach can be applied to the learning based classification results.

Disclaimer

The methods and information presented in this paper are based on research and are not commercially available.

References

[1] Joep Perk et al., "European guidelines on cardiovascular disease prevention in clinical practice (version 2012)," *International journal of behavioral medicine*, vol. 19, no. 4, pp. 403–488, May 2012.

[2] Kenneth Dickstein et al., "ESC Guidelines for the diagnosis and treatment of acute and chronic heart failure 2008," *European Journal of Heart Failure*, vol. 10, no. 10, pp. 933–989, 2008.

[3] Anoop Shetty et al., "A comparison of left ventricular endocardial, multisite, and multipolar epicardial cardiac resynchronization: an acute haemodynamic and electroanatomical study," *Europace*, vol. 16, no. 6, pp. 873–879, February 2014.

[4] Taehoon Shin et al., "Rapid single-breath-hold 3D late gadolinium enhancement cardiac MRI using a stack-of-spirals acquisition," *Journal of Magnetic Resonance Imaging*, vol. 40, no. 6, pp. 1496–1502, December 2014.

[5] Raymond J Kim et al., "The use of contrast-enhanced magnetic resonance imaging to identify reversible myocardial dysfunction," *New England Journal of Medicine*, vol. 343, no. 20, pp. 1445–1453, November 2000.

[6] Engin Dikici et al., "Quantification of Delayed Enhancement MR Images," in *Medical Image Computing and Computer-Assisted Intervention–MICCAI 2004*, pp. 250–257. Springer, September 2004.

[7] Dong Wei, Ying Sun, Ping Chai, Adrian Low, and Sim Heng Ong, "Myocardial Segmentation of Late Gadolinium Enhanced MR Images by Propagation of Contours from Cine MR Images," in *Medical Image Computing and Computer-Assisted Intervention–MICCAI 2011*, pp. 428–435. Springer, September 2011.

[8] Qian Tao et al., "Automated Left Ventricle Segmentation in Late Gadolinium-Enhanced MRI for Objective Myocardial Scar Assessment," *Journal of Magnetic Resonance Imaging*, November 2014.

[9] Tanja Kurzendorfer et al., "Automated Left Ventricle Segmentation in 2-D LGE-MRI," in *Proceedings of the 2017 IEEE International Symposium on Biomedical Imaging: From Nano to Macro*, IEEE, Ed., April 2017, pp. 831–834.

[10] Tanja Kurzendorfer et al., "Random Forest Based Left Ventricle Segmentation in LGE-MRI," in *International Conference on Functional Imaging and Modeling of the Heart*. Springer, June 2017, pp. 152–160.

[11] Pablo Marquez-Neila et al., "A morphological approach to curvature-based evolution of curves and surfaces," *IEEE Transactions on Pattern Analysis and Machine Intelligence*, vol. 36, no. 1, pp. 2–17, January 2014.